Application of Fiber Bragg Grating Sensor for Localized Cryogenic Temperature Measurements

R. Rajini-Kumar[1], M Süßer, H Neumann
Institute of Technical Physics, Forschungszentrum Karlsruhe GmBH, Karlsruhe, Germany

Abstract

Optical method for the evaluation of temperature distribution of multilayer insulation is presented. Five fiber arrays with 4 Fiber Bragg Grating (FBG) sensors in each array are fabricated in a wavelength division-multiplexing (WDM) scheme. MLI temperature varies the gratings periods of the FBG sensors which changes the back reflected Bragg wavelength. This can be correlated with temperature change. For demonstration, a test chamber (219mm Ø X 1900 H) insulated with aluminized Mylar (6* 4 = 24) layer is used. The axial and transverse temperature distribution of MLI is recorded for various vacuum levels. The results obtained were well agreed with the already reported theoretical calculations.

Keywords *(A) Superconductor (D) Temperature sensors (D) Calibration*

1. Introduction

Future space programs and missions require efficient delivery of large payloads over great distances, necessitating the use of high-energy cryogenic upper stages. Therefore, managing the cryogenic fluid, including efficient and reliable insulation materials, is a crucial part of future space exploration. Insulation is a key element in long-duration missions requiring cryogenic storage since relatively small heat fluxes can result in significant boil off losses, increased tank pressure, and increased liquid saturation conditions. Considerable theoretical works have been carried out to understand these complex physical phenomenons's associated with MLI [1]. Some of them attack the problem analytically to give only upper bounds for temperature and pressure in MLI. Recently developed numerical codes are ambitious and advocate complete temporal and spatial information in terms of temperature and pressure developed in the MLI. Even though theoretical analyses seem to be very promising, they lack experimental validation. Most of the codes developed for simulation are one dimensional [2]. Also, several assumptions are made for the modeling of the insulation system in order to simplify the computer simulation which takes it away from the practical system.

The major limitation to validate the theoretical analyses with experiments on the MLI is the unavailability of a suitable sensor that can be integrated effectively during assembly of the MLI for accurate and reliable measurements. The sensor technology, currently available, cannot be used to measure the temperature and pressure distribution (TPD) in MLI. These sensors need penetration of the electrical cabling inside the MLI which may interfere with its thermal performance. Moreover, to measure the TPD, more sensors are required to be installed and this makes the sensing system more complex and costly. Furthermore such standard temperature sensors are bigger in size and therefore they disturb the temperature profile through the layers.

Fiber Bragg Gratings (FBG) is a sensor which works on the principle of wavelength reflection due to the change in the grating length. Gratings with different spatial period are arranged at various positions along a single mode fiber inside the coil. MLI temperature / pressure will vary the gratings' periods, which can be read out with a tunable laser in a wavelength division multiplexing (WDM) scheme. The spectral position of the reflections may be correlated with the spatial position of the gratings, and the shift of the gratings' maximum reflection indicates the change of the gratings' periods, which in turn measures temperature or pressure. Use of FBG sensors is very appealing for sensing the TPD in MLI because of their miniature size and the possibility of having many sensors in a single fiber. This is done by wavelength division multiplexing (WDM) scheme. The temperature profiles throughout the layers are not disturbed due to the very small dimensions (125 μm Ø) of the sensors and the heat conduction is very low when compared to the other standard sensors.

2. FBG Theory

Hill and co workers first observed fiber photosensitivity in germanium-doped silica fiber in 1978 [3]. Meanwhile an entire class of in-fiber components, called the Fiber Bragg Grating (FBG), has been

introduced. Basically, FBG consists of a periodic modulation of the index of refraction along the fiber core, as shown in Figure 1. Ultraviolet (UV) laser light can be used to write the periodic modulation directly into photosensitive fibers. An FBG functions like a filter when a broad-band light is transmitted into the fiber core, reflecting light at a single wavelength, called the Bragg wavelength. Thus, a single wavelength is filtered in the transmitted light spectrum. UV-written in-fiber grating technology has developed very rapidly in recent years and, with gratings now commercially available, FBG is important in telecommunications applications and has great potential in the optical fiber sensor field. FBG as a sensor is compact, simple and can be demodulated in a wavelength-coding manner [3]. FBGs have been considered suitable for measuring static and dynamic fields, such as temperature, strain, and pressure [3].

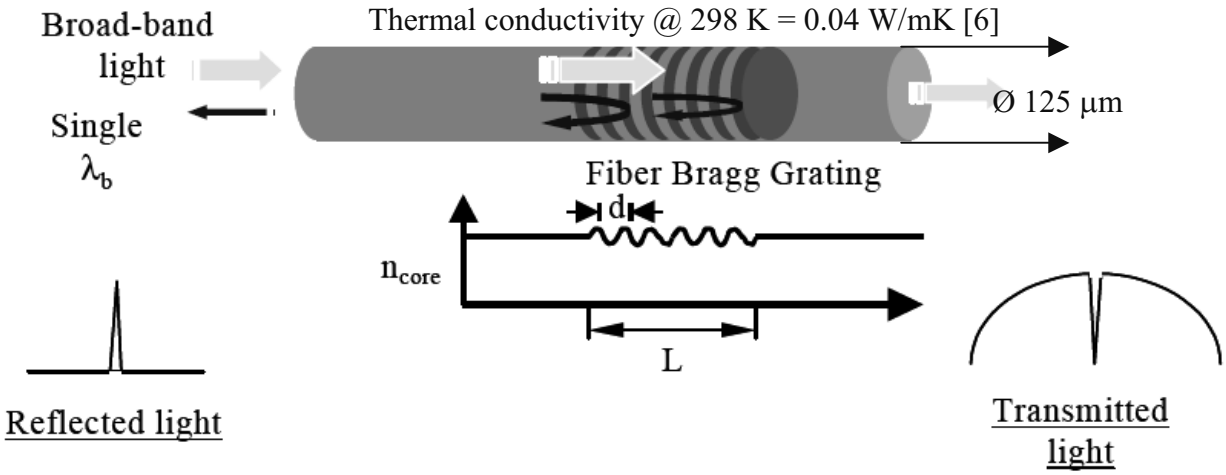

Figure 1 Principle of Fiber Bragg Gratings

When an FBG is expanded or compressed, its grating spectral response is changed. The Bragg reflection wavelength λ_B of an FBG is given as [4]

$$\lambda_B = 2n_{eff}\,d \tag{1}$$

Where the Bragg grating wavelength, λ_B, is the free space center wavelength of the input light will be back reflected from the Bragg grating, n_{eff} is the effective refractive index of the fiber core at the free space center wavelength, and d is the grating spacing.

The Bragg grating resonance, which is the center wavelength of back –reflected light from a Bragg grating, depends on the effective index refraction of the core and the periodicity of the grating. The effective index of refraction, as well as the periodic spacing between the grating planes, will be affected by changes in strain and temperature. Using equation (1) the shift in the Bragg grating center wavelength due to strain and temperature changes is given by

$$\Delta\lambda_B = 2\left(d\frac{\partial n_{eff}}{\partial l} + n_{eff}\frac{\partial d}{\partial l}\right)\Delta l + 2\left(\Lambda\frac{\partial n_{eff}}{\partial T} + n_{eff}\frac{\partial d}{\partial T}\right)\Delta T \tag{2}$$

The first term in equation 2 represents the strain effect on an optical fiber. This corresponds to a change in the grating spacing and the strain-optic induced change in the refractive index. The above strain effect term may be expressed as [4]

$$\Delta\lambda_B = \lambda_B\left(1 - p_e\right)\varepsilon_z \tag{3}$$

where p_e is an effective strain – optic constant defined as

$$p_e = \frac{n_{eff}^2}{2}\left[p_{12} - \nu\left(p_{11} + p_{12}\right)\right] \tag{4}$$

p_{11} and p_{12} are components of the strain –optic tensor, and v is the Poisson's ratio. For temperature measurement this term is kept constant.

The second term in equation 2 represents the effect of the temperature on an optical fiber. A shift in the Bragg wavelength due to thermal expansion changes the grating spacing and the index of refraction. This fractional wavelength shift for a temperature change ΔT may be written as [4]

$$\Delta\lambda_B = \lambda_B(\alpha_d + \alpha_n)\Delta T \tag{5}$$

Where $\alpha_d = \left(\frac{1}{d}\right)\left(\frac{\partial d}{\partial T}\right)$ is the thermal expansion coefficient for the fiber (approximately 0.55 * 10^{-6} for silica).

$\alpha_n = \left(\frac{1}{n_{eff}}\right)\left(\frac{\partial n_{eff}}{\partial T}\right)$ is thermo-optic coefficient, (~ 8.6 * 10^{-6} for the germania-doped, silica –core fiber).

2.1 Strain cross sensitivity:

From equation 2 it is clear that the change in the Bragg wavelength is the result of both temperature and strain effects. In order to measure the MLI temperature distribution using FBG sensors with high accuracy, the strain effect has to be cancelled. Hence during installation the FBG sensors are left hanging free near the walls of the intermediate MLI, shown in figure 2, to ensure that the sensors did not experience any physical stress. By this way, it can be assured that the change in the Bragg wavelength is purely due to temperature.

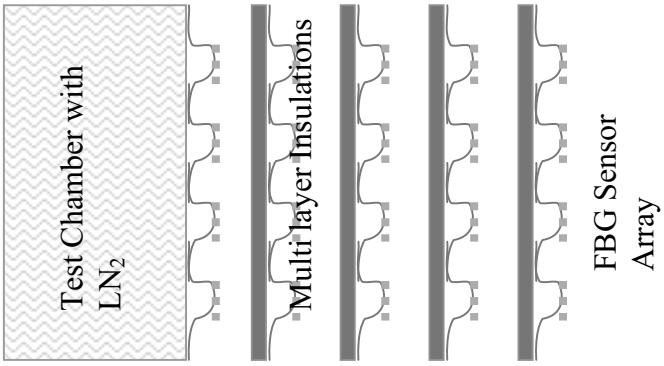

Figure 2: FBG sensor array installation for avoid strain effects and to measure temperature distribution accurately.

3. Sensor design and calibration.

Corning single mode fiber (SMF 28) has been used to fabricate the FBG sensing arrays. Five FBG sensor arrays are fabricated with four individual sensing elements in each array. These sensing elements are fabricated with different Bragg wavelength, which will enable the instrumentation setup to measure all the sensors simultaneously using wavelength division multiplexing (WDM) scheme. Figure 3 shows the scheme of the sensor design for MLI temperature measurements. The sensor elements are placed at equal distance in 1.5 m length fiber. This helps to locate the position of the sensors inside the MLI after installation. The fabricated sensors are then calibrated with the 2 point calibration method. The FBG sensors arrays are dipped directly into the Liquid nitrogen tank and then the change in the Bragg wavelength has been recorded. A calibrated PT 100 temperature sensor is used for reference and for the FBG sensors calibration. The average sensitivity of the sensor is calculated to be 17 pm / K. A linear fit equation is used to convert the Bragg wavelength shift into corresponding temperature.

4. Experimental setup

Test chamber (219mm Ø X 1900 H) insulated with aluminized Mylar (6* 4 = 24) layer is used to measure the temperature distribution in the test module with warm boundary at room temperature and cold boundary at 77 K is shown in Figure 4. The arrangement of WDM FBG sensors in the insulation

layers are also shown in Figure 4. All the FBG sensor arrays are then combined together which then connected to the optical spectrum analyzer and to the light source. A broadband ELED (edge light emitted diode) light source with a central wavelength of 1550 nm is used for powering the FBG sensor arrays. The ELED has a FWHM (Full Width at Half Maximum) line width of 45 nm and a peak light power of 45μW.

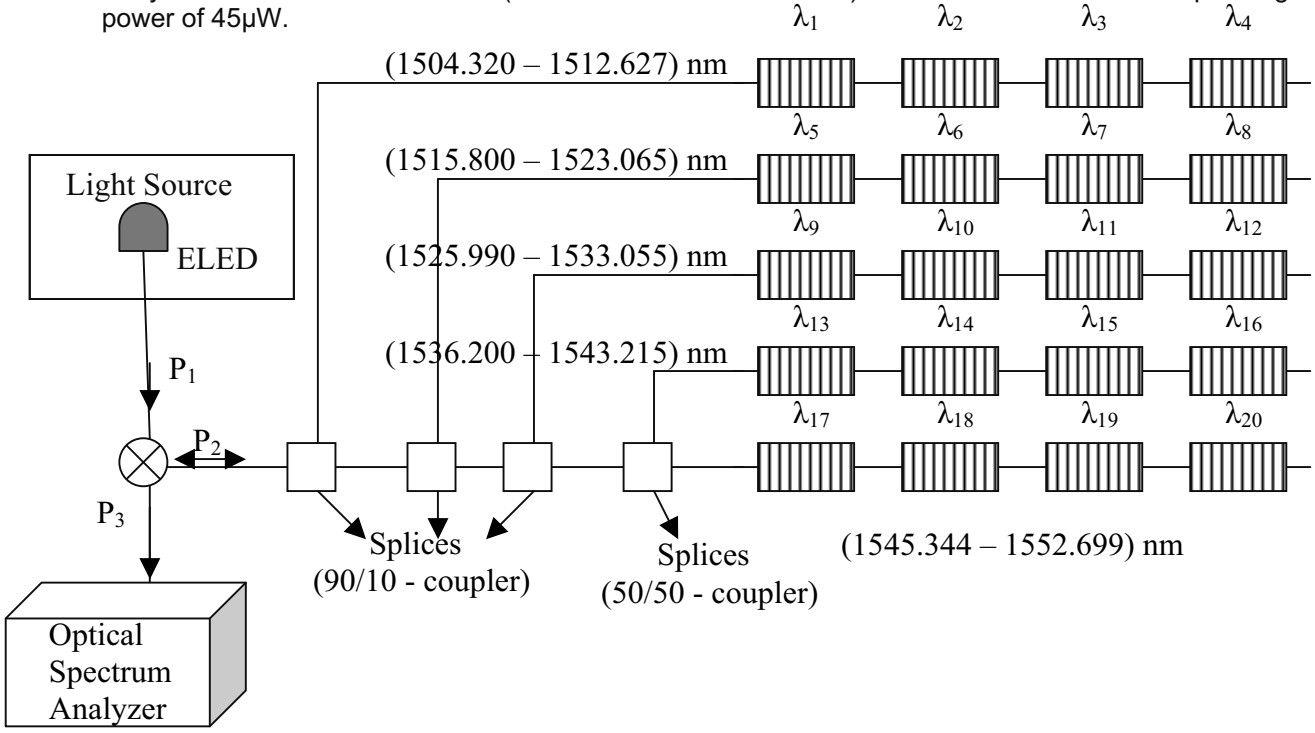

Figure 3 Sensor design concept

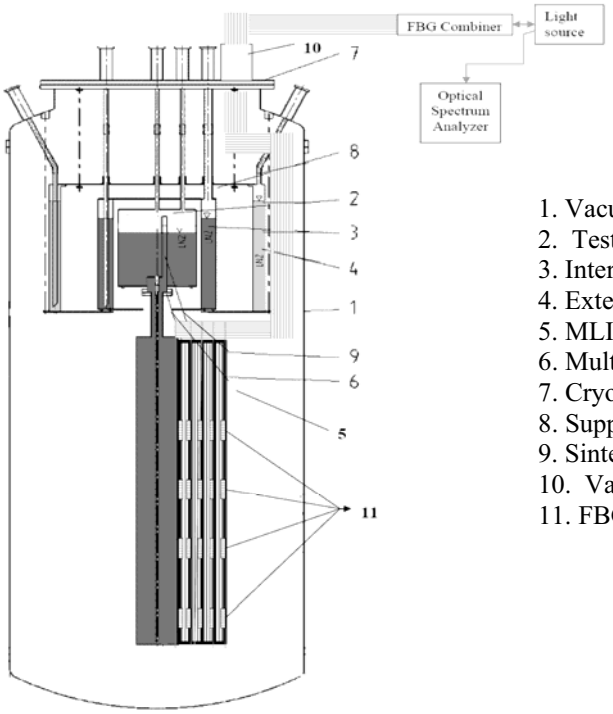

1. Vacuum tank
2. Test Chamber
3. Intermediate guard chamber
4. External LN_2 Guard
5. MLI
6. Multi interface flange
7. Cryostat lid
8. Support plate
9. Sintered element
10. Vacuum tight Fiber feed through
11. FBG sensors

Figure 4 MLI Transverse and axial temperature distribution measurement setup

The light source, integrated with the circulator is powered by DC voltage rating of 12 V / 400 mA. Figure 5 shows the measurement principle of the FBG sensors. The LED driver drives a constant current through a pigtailed LED. The light enters the circulator from the ELED light source through port 1 (P_1) and exits through port 2 (P_2). The reflected light from the FBG sensors enters port 2 (P_2) and exits through port 3 (P_3). Since the optical circulator is an inherently non-reciprocal device, the light

never goes to other ports. Through the circulator P_3, the reflected light is captured with an AQ8317B Optical spectrum analyzer. After the sensor array installation, the responses of all 20 sensors are recorded to check the survival of the sensors and to ensure the proper installation of the sensors.

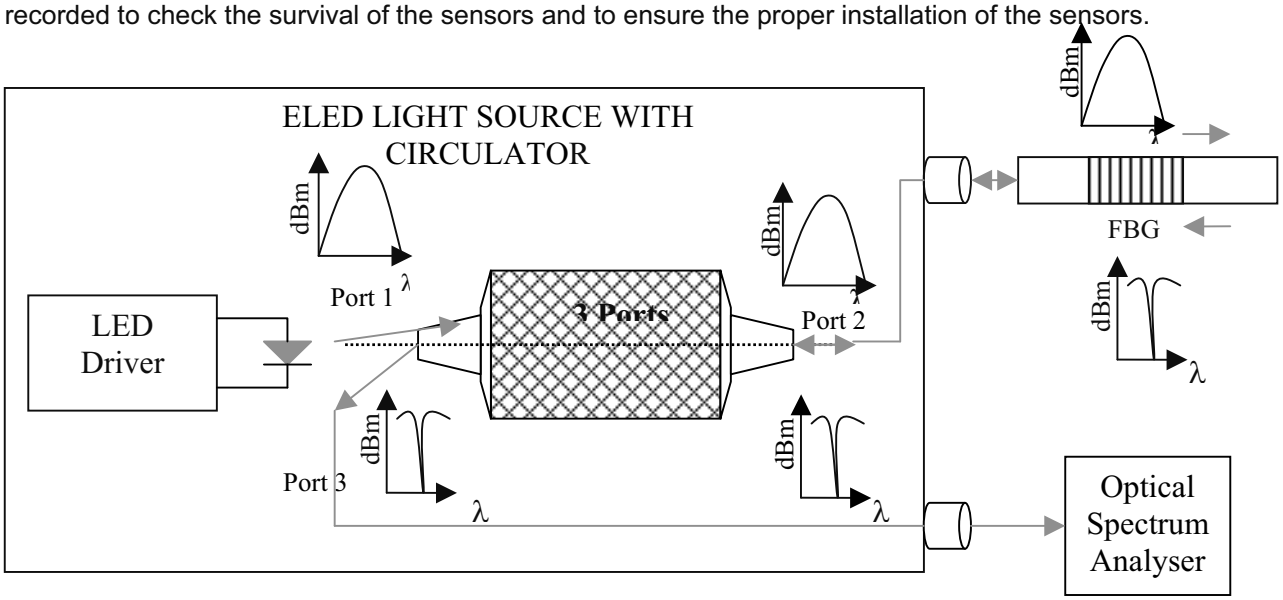

Figure 5. FBG sensor – Measurement principle

5. Experiment Conduction

After the FBG sensor installation, the test chamber is kept inside the cryostat and the vacuum is created in steps and cooled down to 77 K. Finally vacuum of 3.4 * 10^{-6} m bar is maintained in the test chamber. The test chamber is then guarded by the intermediate guard chamber filled with LN_2, which in turn guarded by the external LN_2 guard chamber to ensure the zero LN_2 loss. The temperature distributions are recorded using the optical spectrum analyzer which is then compared with the calculated theoretical temperature taken from Neumann [5]. Figure 7 -10 shows the measured transverse and axial temperature distributions in MLI for various vacuum levels and the averaged temperatures of MLI.

6. Results and Discussion

Figure 6 shows the temperature distribution in the MLI for various vacuum levels. From figure 6 it is clear that, to get a good insulation, the vacuum level should be in the order of 10^{-3} to $10^{-6.}$ Also from figure 7, it can be seen that the insulation quality of the MLI for 3 hrs, 24 hrs and 48 hrs along with averaged temperature distribution of MLI. It is clear that the insulation quality is maintained without any degradation once it gets stabilized. More over, it is observed from figure 7 that the measured temperature is well coincide with the calculated temperatures. But a small difference between the measured and calculated values of ~ ±1.5 K is observed. This is because the sensors are not fixed firmly to the layers, but it is left hanged in between the layers to avoid the mechanical stresses in the sensors. The missing contact between the sensors and the layers is one important reason for the difference between the measured and calculated values. The sensor sensitivity is calculated to be 18.9 nm / K. From the above results, it is evident that the FBG sensors could be the right choice to study the thermal performance of the MLI. In future, the sensors will be fixed on the layers to get more accurate measurements.

ACKNOWLEDGEMENTS
I thank Mr. Seidler (ITP / FZK) for helping me in conducting the experiments.

REFERENCES

1. Bapat, S. L., Narayankhedkar, K. G., Lukose, T. P., Performance Predictions of Multilayer Insulation, Cryogenics, Vol. 30, August 1990, p. 700-710
2. MacGregor, R. K., Pogson, J. T., Russell, D. J., Numerical Evaluation of Multilayer Insulation System Performance, AIAA Paper, No. 70-848
3. Raman Kashyap “Fiber Bragg Gratings”, Academic press, 1999

4. Othonos A, Kalli K, “Fiber Bragg Gratings – Fundamentals and application in telecommunications and sensing”, Artech House optoelectronics library, 1999
5. Neumann H., Concept for thermal insulation arrangement within a flexible cryostat for HTS power cables „Cryogenics 44 (2004) 93–99.
6. http://www.engineeringtoolbox.com/thermal-conductivity-d_429.html

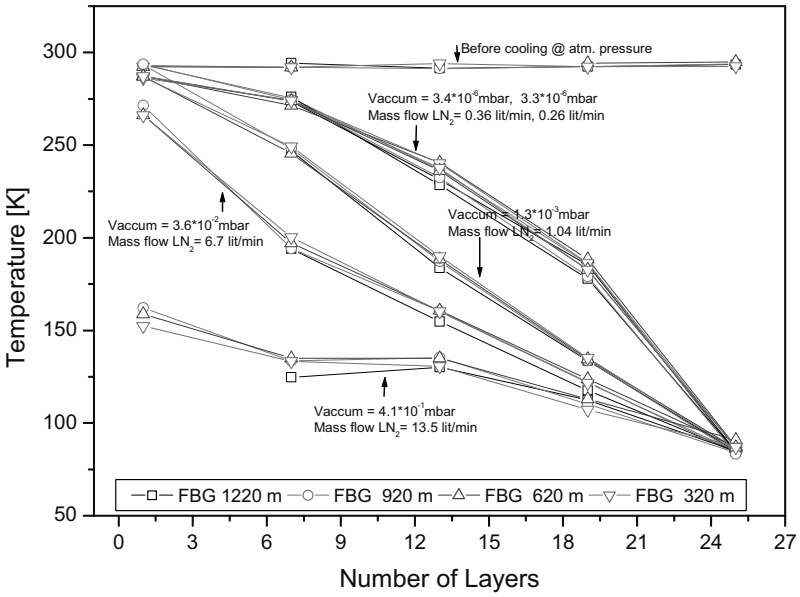

Figure 6 Transverse temperature distribution in the MLI for various vacuum levels (20 sensors)

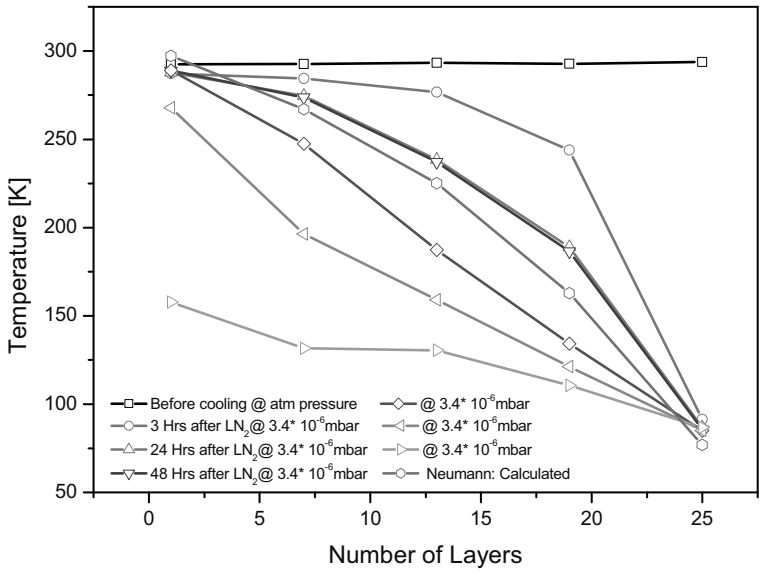

Figure 7 Averaged transverse temperature distribution in the MLI for various vacuum levels